

## Errata

**Document Title:** Dielectric Measurements With Time Domain Reflectometry  
(AN 118)

**Part Number:** 5952-1768

**Revision Date:** March 1970

---

### HP References in this Application Note

This application note may contain references to HP or Hewlett-Packard. Please note that Hewlett-Packard's former test and measurement, semiconductor products and chemical analysis businesses are now part of Agilent Technologies. We have made no changes to this application note copy. The HP XXXX referred to in this document is now the Agilent XXXX. For example, model number HP8648A is now model number Agilent 8648A.

### About this Application Note

We've added this application note to the Agilent website in an effort to help you support your product. This manual provides the best information we could find. It may be incomplete or contain dated information, and the scan quality may not be ideal. If we find a better copy in the future, we will add it to the Agilent website.

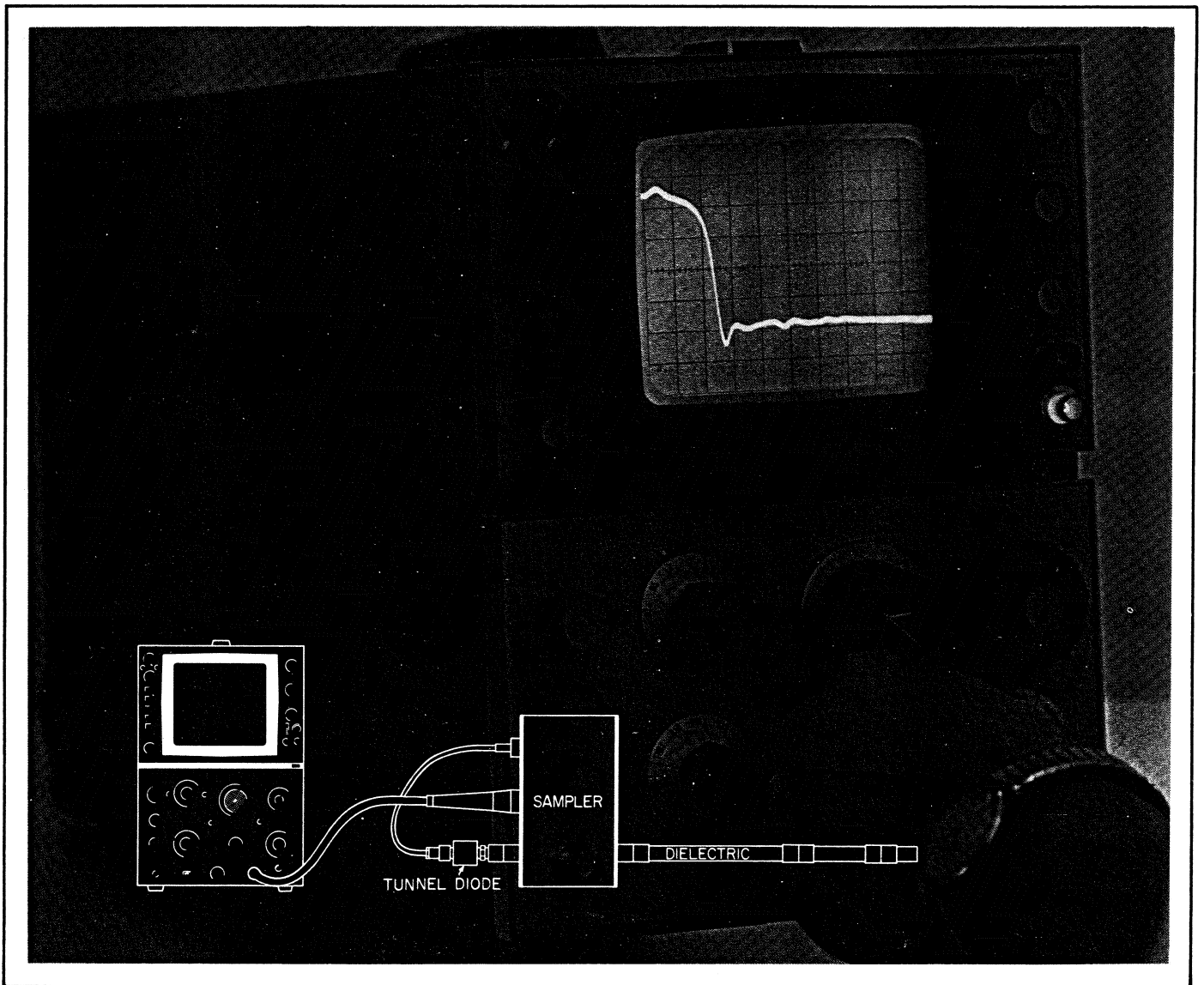
### Support for Your Product

Agilent no longer sells or supports this product. You will find any other available product information on the Agilent website:

[www.agilent.com](http://www.agilent.com)

Search for the model number of this product, and the resulting product page will guide you to any available information. Our service centers may be able to perform calibration if no repair parts are needed, but no other support from Agilent is available.

# DIELECTRIC MEASUREMENTS WITH TIME DOMAIN REFLECTOMETRY



## FOREWORD

This application note has been prepared for chemists, physicists, and electronic engineers. The quite different background of these readers requires detailed treatment of the subject to make it understandable to everyone. On the other hand, going into too much detail would impair the ease of reading. We have compromised by adding two appendices, one on Laplace transforms which are less familiar to the chemist, and one on the theory of dielectrics which may be of interest to electronic engineers and physicists.



APPLICATION NOTE 118

DIELECTRIC MEASUREMENTS  
WITH  
TIME DOMAIN  
REFLECTOMETRY

**TABLE OF CONTENTS**

|   | Page |
|---|------|
| SECTION   |      |
| 1. Introduction . . . . .   | 1    |
| 2. Basic Relations For The Measurement<br>Of Dielectric Properties With TDR . . . . . | 1    |
| 3. Practical Aspects Of The TDR<br>Measurements . . . . .                             | 8    |
| APPENDIX I  |      |
| The Correlation Between Time and<br>Frequency Domain . . . . .                        | 13   |
| APPENDIX II   |      |
| The Principle of Dielectric Measurements . . . . .                                    | 16   |

## 1. INTRODUCTION.

The measurement of the dielectric behavior of solids and liquids is of practical and theoretical interest to engineers, chemists, and physicists. Electronic engineers are interested in the dielectric constant and loss of materials at certain frequencies for RF and microwave applications. Chemists and physicists obtain important information, from such measurements, about molecular structure, particularly in polymers and solvent-solute systems.

Generally the measurements are made by placing the substance between two plates of a capacitor (at low frequencies) or in a coaxial line and measuring the complex impedance. A number of measurements over a wide frequency range is required for complete characterization, which is time consuming and demands a considerable investment in instrumentation, particularly for the microwave region. Therefore, in spite of its usefulness, this method has found rather limited applications. However, one can obtain the same information over a wide frequency range in only a fraction of a second by making the measurement not in the frequency domain but in the time domain, using a pulse that simultaneously contains all the frequencies of interest. This pulse method has been used for low frequency investigations on dielectrics. Modern tunnel diode pulse generators and wide band sampling oscilloscopes extend this method into the microwave region where savings in time and equipment are most pronounced.

## 2. BASIC RELATIONS FOR THE MEASUREMENT OF DIELECTRIC PROPERTIES WITH TDR.

The time domain reflectometer consists of a pulse generator which produces a fast rise time step, a sampler which transforms a high frequency signal into a lower frequency output, and an oscilloscope or any other display or recording device (see Figure 2.1).

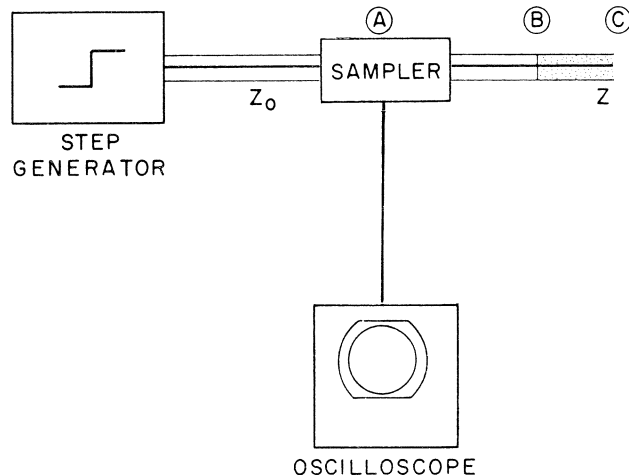


Figure 2.1 Time domain reflectometer setup.

The pulse from the step generator travels along the coaxial line until it reaches the point A. The sampler detects and the oscilloscope displays the voltage step (A) as it travels past point A (see Figures 2.1 and 2.2). The coaxial line which transmits the pulse has a characteristic impedance of 50 ohms ( $Z_0 = 50$  ohms). Whenever there is a discontinuity in this line, a fraction of the traveling wave is reflected back to the generator. Therefore, at the interface of the 50 ohm line with any other impedance  $Z$  (point B) part of the step pulse is reflected and passes point A again, producing an additional signal (B) which is displayed on the oscilloscope. The time elapsed between the first and second step is equal to the transit time of the traveling wave from A to B and back to A again.

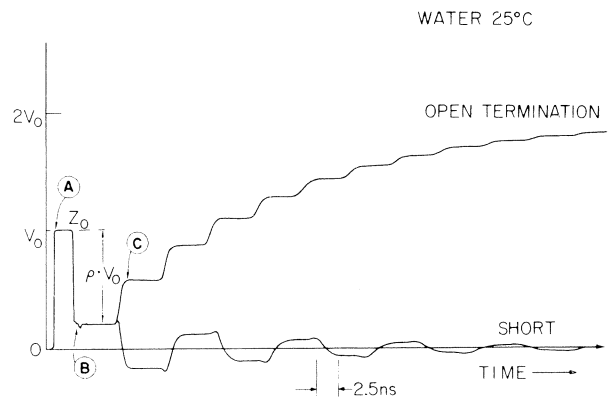


Figure 2.2 Typical TDR reflection from dielectric sample. (See text.)

The remainder of the wave, which was not reflected at B, travels to C. If we terminate the line at C with an open end then all of the wave is reflected back in phase (assuming no losses due to radiation). Part of this pulse is reflected again at B and part of it goes through past A, giving rise to another step (C). The time between step (B) and (C) is the transit time from B to C and back to B again.

The multiple reflections between B and C continue until all of the pulse energy has been reflected and absorbed by the generator. If we use a short at C as a termination, then an incident wave is totally reflected again, but  $180^\circ$  out of phase, and the multiple reflections reduce the signal at A until it reaches zero. The first reflection at B, however, is completely independent of the termination at C.

There are different types of Hewlett-Packard time domain reflectometers with risetimes from 35 to 150 ps to fit every need and budget. They are built for the 140 series or the 180 series plug-in oscilloscopes. The presently available combinations and some of their operating characteristics are shown

in Figs. 2.3 and 2.4. Representative set-ups for the 140A and 180A oscilloscope, both with 35 ps risetime, are shown in Figures 2.5a and 2.5b. With an analog-to-digital converter it can be tied to and programmed from a computer for immediate conversion of the reflection coefficient into permittivity.

The magnitude of the first step,  $V_o \cdot \rho$ , is

$$V_o \cdot \rho = V_o \frac{Z_o - Z}{Z + Z_o} \quad \begin{array}{l} \rho : \text{reflection coefficient} \\ V_o : \text{pulse height} \end{array} \quad (2.1)$$

and the characteristic impedance  $Z$  of a coaxial line

$$Z = \frac{60}{\sqrt{\kappa}} \ln \frac{D}{d} \quad \begin{array}{l} D : \text{diameter of outer conductor} \\ d : \text{diameter of inner conductor} \\ \kappa : \text{permittivity} \end{array} \quad (2.2)$$

An empty coaxial line with the impedance  $Z_o$  will have a smaller impedance  $Z$  when filled with a dielectric of the permittivity  $\kappa$ ,

$$Z = \frac{Z_o}{\sqrt{\kappa}} \quad (2.3)$$

Thus, the reflection coefficient  $\rho$  is a function of  $\kappa$ :

$$\rho = \frac{1 - \sqrt{\kappa}}{1 + \sqrt{\kappa}} \quad (2.4)$$

and

$$\kappa = \left( \frac{1 - \rho}{1 + \rho} \right)^2 \quad (2.5)$$

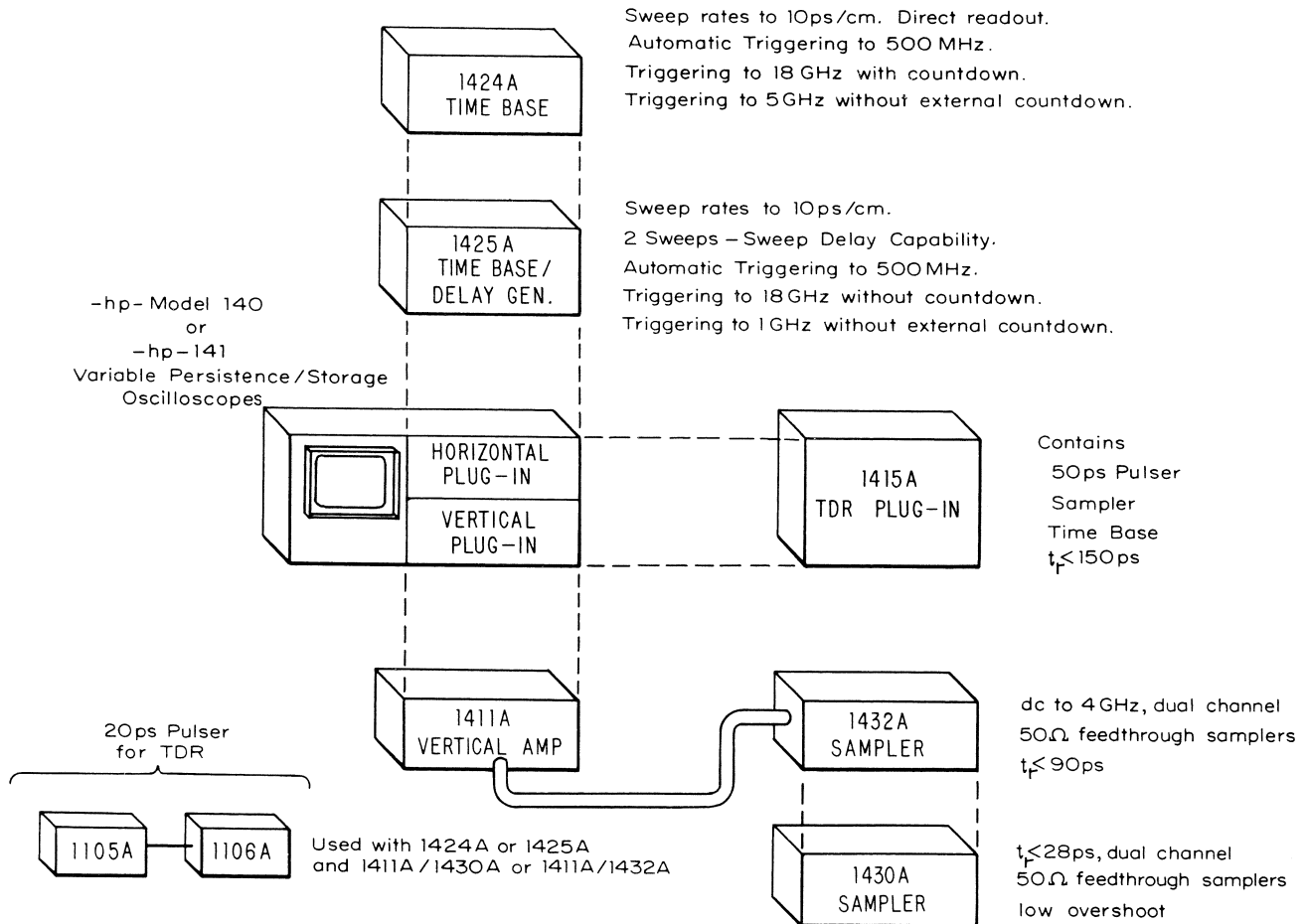


Figure 2.3 HP 140 System with either 1415A 130 ps risetime TDR plug-in or with 35 ps risetime TDR plug-ins and samplers.

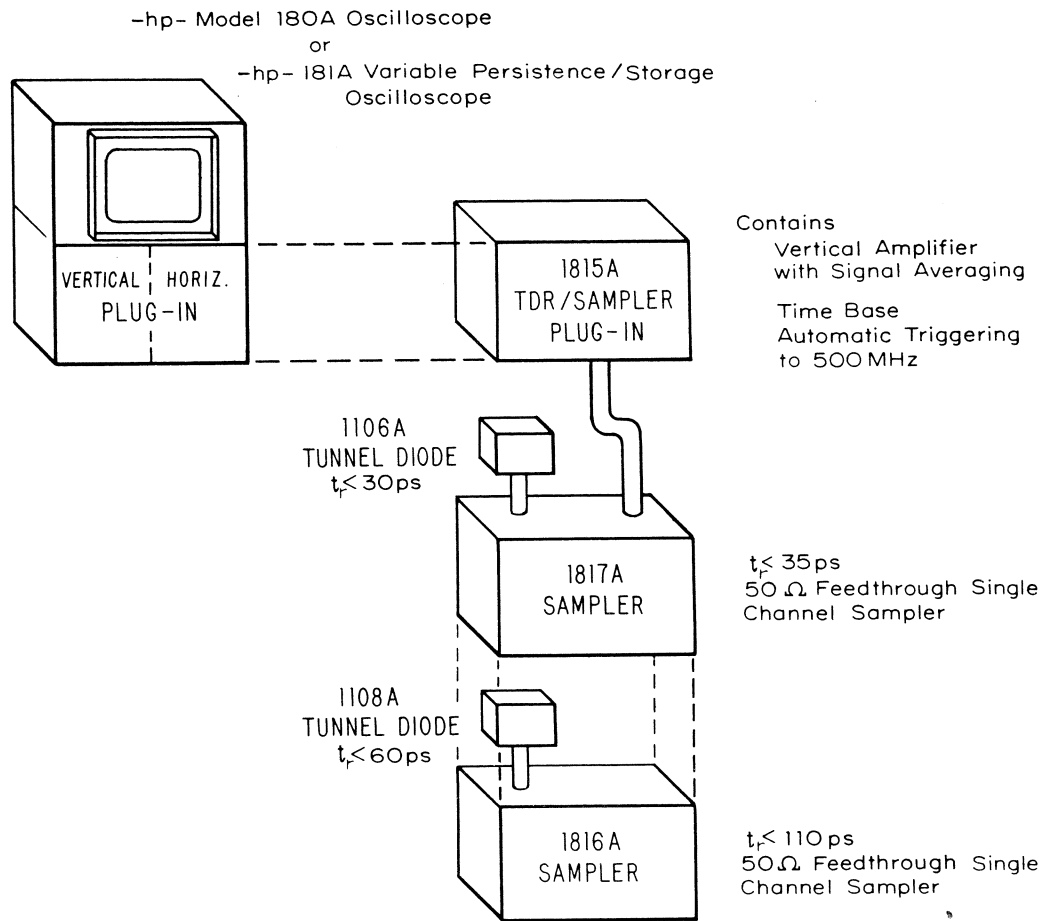


Figure 2.4 HP 180 System with 1815A 35 ps risetime calibrated TDR.

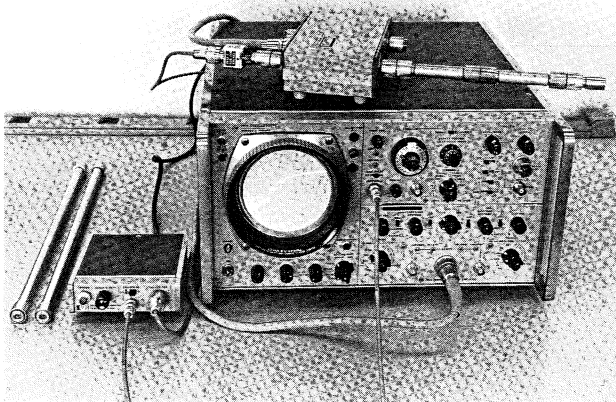


Figure 2.5a HP 140 System with 35 ps risetime.

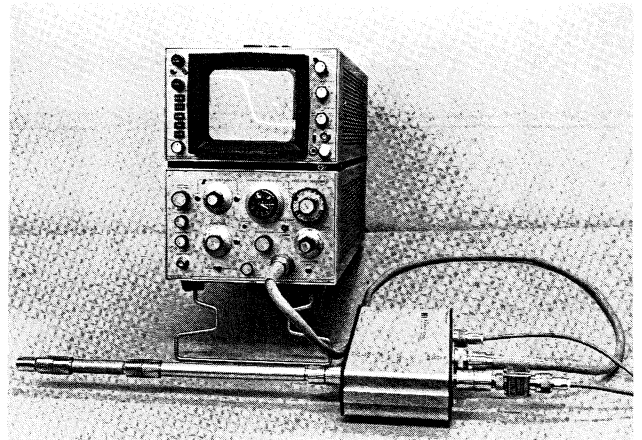


Figure 2.5b HP 180 System with calibrated 35 ps risetime.

The equivalent circuit for a coaxial line, without and with dielectric is shown in Figure 2.6, corresponding to a characteristic impedance

$$Z_0 = \sqrt{\frac{L}{C'}} \quad (2.6)$$

and

$$Z(\omega) = \sqrt{\frac{j\omega L + R}{j\omega\kappa^*C' + G_0}} \quad (2.7)$$

$G_0$  : low frequency conductance per unit length

with

$$\kappa^* = \kappa_\infty + \frac{\kappa_0 - \kappa_\infty}{1 + j\omega\tau} \quad \kappa_0 : \text{low frequency permittivity} \quad (2.8)$$

(see Appendix II)

$\kappa_\infty$  : high frequency permittivity

$\tau$  : relaxation time

$$\kappa(t) = \kappa_\infty + (\kappa_0 - \kappa_\infty) (1 - e^{-\frac{t}{\tau}}) \quad (2.9)$$

for ideal dielectrics. In most applications with reasonable lengths of transmission lines  $R \approx 0$ . In equation 2.7, the low frequency conductance  $G_0$  is assumed to be frequency independent. Actually, the conductivity  $\sigma$  drops to zero at high frequencies in all ionic conductors and often  $G_0$  can be neglected. The conductance and conductivity are related by

$$\frac{G_0}{C'} = 4\pi\sigma \quad [\Omega^{-1} \text{cm}^{-1}] = \frac{4\pi\sigma}{1.1 \cdot 10^{-12}} \quad [\text{sec}^{-1}] \quad (2.10)$$

since

$$G_0 = \frac{2\pi\sigma}{\ln \frac{D}{d}} \quad \text{and} \quad C' = \frac{1}{2 \ln \frac{D}{d}}$$

Therefore Z becomes

$$Z(\omega) = \sqrt{\frac{j\omega L}{j\omega\kappa^*C' + \frac{4\pi\sigma}{1.1 \cdot 10^{-12}}}} \quad (2.11)$$

$$= Z_0 \sqrt{\frac{1}{\kappa^* - j \frac{4\pi\sigma}{\omega \cdot 1.1 \cdot 10^{-12}}}}$$

and for

$$\frac{4\pi\sigma}{1.1 \cdot 10^{-12} \omega} \ll \kappa'' \quad (2.12)$$

$$Z(\omega) = \frac{Z_0}{\sqrt{\kappa^*}}$$

which was already used in equation (2.3).

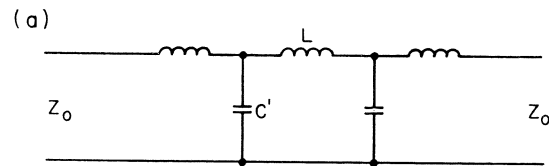
The complex permittivity in the frequency domain  $\kappa^*(\omega) = \kappa' - j\kappa''$   $\kappa^*(\omega)$  : frequency dependency of the complex permittivity of the medium between conductors

can be transformed into the time domain by Laplace transform:

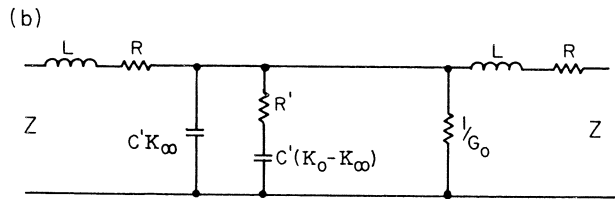
$$\kappa(t) = \frac{1}{2\pi} \int_{-\infty}^{+\infty} \kappa^*(\omega) e^{i\omega t} d\omega$$

$\kappa(t)$  : time function of the permittivity

(see Appendix I and II).



LOSSLESS COAXIAL LINE



$R'C'(K_0 - K_\infty) = \tau$   
COAXIAL LINE WITH IDEAL DIELECTRIC

Figure 2.6 Equivalent circuit of a coaxial line with and without dielectric.

We now see that the impedance Z, and therefore the reflection coefficient  $\rho$  are functions of the permittivity  $\kappa^*$ , both in the frequency and time domain. A time dependence of the permittivity is reflected in a time dependence of the reflection coefficient. The step at (B) in Figure 2.2 is modified depending on the relaxation properties of the dielectric. The measurement is made only at the interface between air and dielectric and undisturbed as long as there are no additional reflections present from any point beyond point B in Figure 2.1. Therefore, the time for the return trip of the wave in the line filled with the dielectric limits the maximum time available for the measurement and is:

$$t [\text{ns}] = \frac{2L\sqrt{\kappa'}}{c} = \frac{\sqrt{\kappa'}}{15} \cdot l [\text{cm}] \quad (2.13)$$

For our application the transformation of the reflection coefficient  $\rho$  has to be made. Thus

$$\rho(t) = \frac{1}{2\pi} \int_{-\infty}^{+\infty} \frac{\sqrt{1 - \kappa^*(\omega)}}{\sqrt{1 + \kappa^*(\omega)}} \cdot e^{j\omega t} d\omega \quad (2.14)$$

This integral cannot be solved in closed form, even for ideal dielectrics, but we have derived expressions for the reflection coefficient as a function of time in the form of infinite series for Debye dielectrics. With the aid of a computer, these series have been used to compute this function for a wide range of cases of practical interest. These results are presented in graphical form in such a way as to facilitate determining the true relaxation time from observed reflected waveforms. Furthermore, several independent determinations of the relaxation time can be made from different features of the reflected waveform. The consistency of the values obtained for a given die-

lectric serves as a powerful check of the correctness of the assumptions underlying the method. The most important of these assumptions is that the dielectric is of the Debye type, having a single relaxation time.

Fig. 2.7 gives an actual plot of the time dependence of the reflection coefficient  $\rho(t)$  of amyl alcohol, recorded from the oscilloscope output with a Moseley X-Y recorder.  $\rho_\infty$  and  $\rho_0$  can be read directly.

The relaxation time  $\tau$  can conveniently be determined from the measured time  $\tau'$  for  $\rho_0 - \rho(t)$  to decrease to some specified fraction of its initial value  $\rho_0 - \rho_\infty$ . Figs. 2.8, 2.9 and 2.10 show  $\tau/\tau'$  as abscissa with  $\kappa_0$  as ordinate for a range of values of  $\kappa_\infty$  practical interest.  $\tau'$  is the time necessary for  $(\rho_0 - \rho(t))/(\rho_0 - \rho_\infty)$  to reach the values 0.8,  $1/\epsilon$ , and 0.2, respectively, in the three figures. Both coordinates are plotted logarithmically. The resulting curves are plotted logarithmically. The resulting curves have relatively little curvature and are nearly parallel to each other over the range plotted.

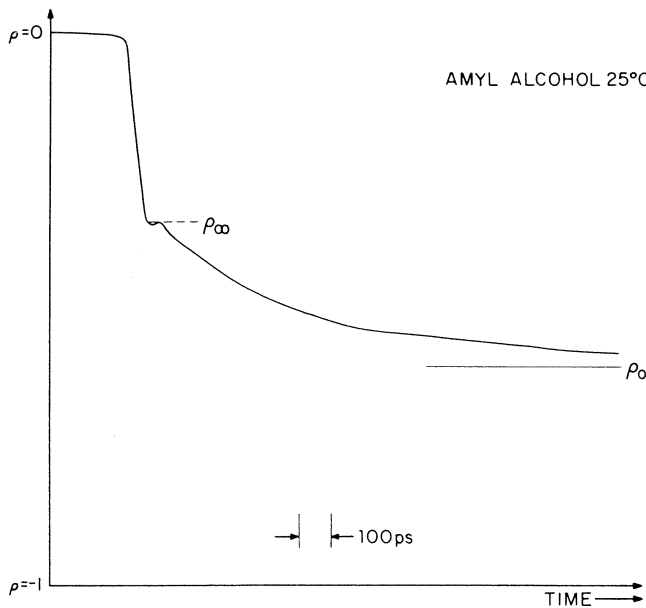


Figure 2.7 Oscilloscope trace of the reflection from the interface amyl alcohol-air.

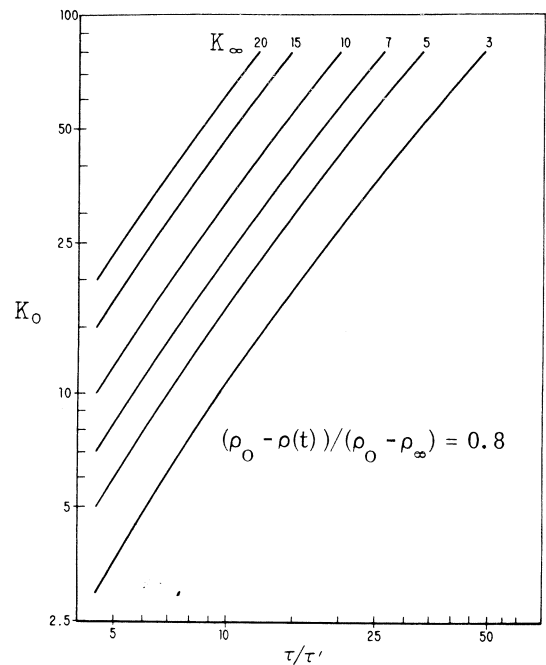


Figure 2.8 Ratio of the true relaxation time  $\tau$  to the measured time  $\tau'$  at the 80% point of the reflection coefficient.

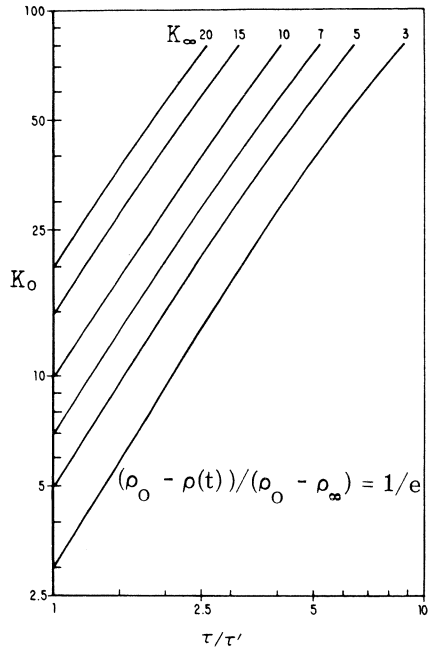


Figure 2.9 Ratio of the true relaxation time  $\tau$  to the measured time  $\tau'$  at the  $1/e$  point of the reflection coefficient.

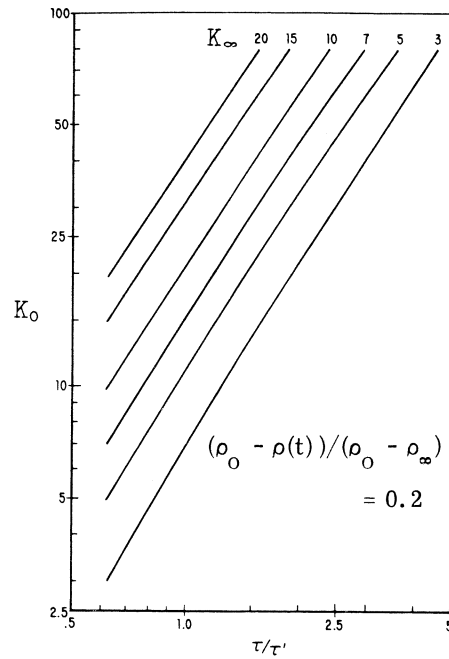


Figure 2.10 Ratio of the true relaxation time  $\tau$  to the measured time  $\tau'$  at the 20% point of the reflection coefficient.

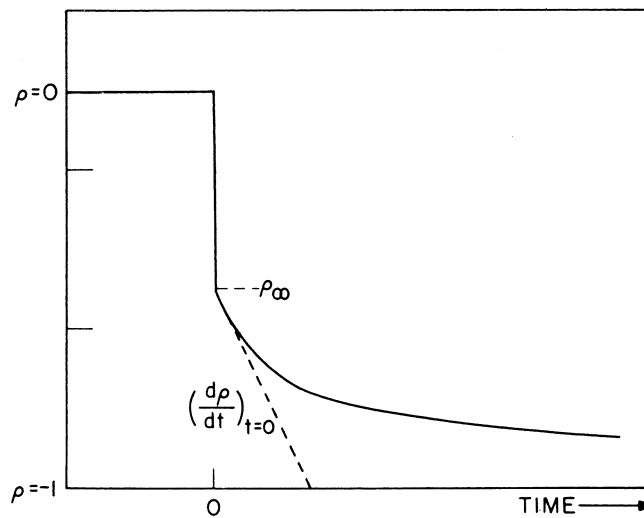


Figure 2.11 Theoretical time dependence of the reflection coefficient for dielectrics with high conductivity, according to Equation 2.15.

We have already mentioned that in most cases ionic conductivity can be neglected at high frequencies. As an example, the imaginary part of the permittivity (loss) in equation (2.12) may be about 5 at  $\omega\tau = 1$ . Assuming  $\omega = 6 \cdot 10^9$  Hz requires that  $\sigma \ll 3 \cdot 10^{-3}$  [ $\Omega^{-1} \text{cm}^{-1}$ ]. Generally dielectric materials (except for highly dissociated solutions of small ions in strongly polar solvents) will have a conductivity in the microsiemens range ( $1\text{S} = 1 \text{ohm}^{-1}$ ) at 1 GHz and the method described above can be used to determine the dielectric properties. On the other hand, if ionic conductivity is predominant, then the reflection coefficient will not level out at a certain value, corresponding to  $\kappa_0$ , but will drop to zero, following the equation(1)

$$\rho(t) = (1 + \rho_\infty) \cdot (I_0(xt) + I_1(xt)) \cdot e^{-xt} \quad (2.15)$$

$$\text{with } x = \frac{G_0}{2\kappa C^2} = \frac{2\pi\sigma}{\kappa}$$

$$\text{and } \rho_\infty = \frac{1 - \sqrt{\kappa}}{1 + \sqrt{\kappa}}$$

Figure 2.11 gives  $\rho(t)$  and Figure 2.12 shows the measured reflection coefficient vs. time of an ionic solution in N-methylformamide. The first step  $\rho_\infty$  gives the dielectric constant at high frequency and the slope at  $t = 0$

$$-\left(\frac{d\rho}{dt}\right)_{t=0} = \frac{G_0(1 + \rho_\infty)}{4\kappa C^2} = \frac{\pi\sigma(1 + \rho_\infty)}{\kappa \cdot 1.1 \cdot 10^{-12}} \quad (2.16)$$

In this example a permittivity  $\kappa = 40$  and a conductivity  $\sigma = 3 \cdot 10^{-2}$  siemens/cm was measured under the assumption that  $\kappa$  remains constant. Such a conductivity makes dielectric constant measurements with other methods at high frequencies quite difficult. With TDR, however, ten times higher conductivities could be determined with ease.

A remark about the accuracy of dielectric measurements with TDR. First, it depends on the mechanical accuracy of the coaxial line used. The standard 7mm precision coaxial air lines have an impedance of  $50 \pm 0.1$  ohms or a maximum deviation of 0.2%. Since

$$\kappa = \left(\frac{Z}{Z_0}\right)^2$$

the relative error in  $\kappa$  can be  $\pm 0.4\%$ .

(1) B.M. Oliver, Hewlett-Packard Journal Vol. 15, No. 6 (1964).

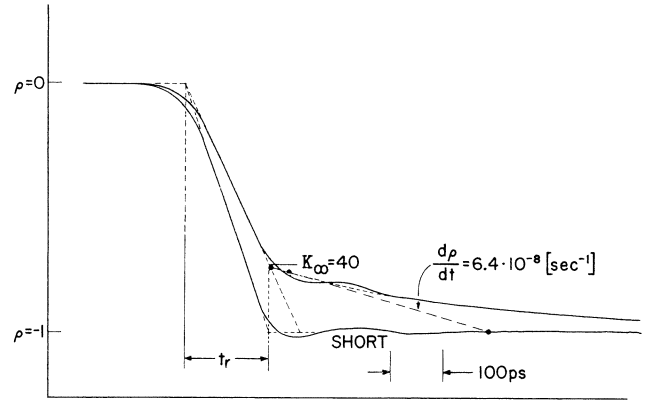


Figure 2.12 Actual reflection from a dielectric with high conductivity (ionic solution in N-methylformamide). The reflection from a short in place of the interface air-dielectric recorded on the same plot to allow correcting some overshooting and ringing of the TDR system pulse response. The method of determining  $\rho_\infty$  is the same as shown in Figure 2.14.

A second source of error is any inaccuracy in the measurement of the reflection coefficient. It may be due to nonlinearity of the amplifier in the oscilloscope or the recorder, which is less than 1%, or due to unwanted reflections from poorly matched transmission lines, including the sampler. Arrangements shown in Part 3 can suppress the latter and allow an over-all measurement accuracy of the reflection coefficient  $\frac{\Delta\rho}{\rho} \leq 0.01$  or  $\Delta\rho \leq 2 \cdot 10^{-3}$  whichever is greater. The transformation of  $\rho$  into  $\kappa$ , however, multiplies this error by a factor

$$\frac{\Delta\kappa}{\Delta\rho} = -\sqrt{\kappa} (1 + \sqrt{\kappa})^2 \text{ and } \frac{\Delta\kappa}{\Delta\rho/\rho} = -(1 - \kappa)\sqrt{\kappa} \quad (2.17)$$

$\Delta\kappa$  is shown in Figure 2.13 for the different sources of error mentioned. The error due to the tolerance in the coaxial line can be reduced to an insignificant amount by measuring the physical dimensions of inner and outer conductors with an accuracy of 0.5 and 1.0  $\mu\text{m}$  respectively. If this is done, the absolute accuracy of the dielectric constant is determined mainly by amplifier nonlinearities, except for the lowest values of  $\kappa$  where noise and unwanted reflections become the limiting factor. Obviously, relative measurements, using a reference sample, can be made with much higher accuracy.

A poorly defined interface between air and dielectric e.g., a liquid meniscus, produces another error that reduces the system risetime or high-frequency cutoff. Imagine an ideal dielectric with no relaxation reflecting a  $\delta$ -function impulse, which contains all frequencies of equal amplitude. The reflected pulse will be a  $\delta$ -function again, if the interface air dielectric is parallel to the electric field. If the interface extends over a certain distance in the

direction of the traveling wave, then the reflected pulse will be spread out, corresponding to the return trip time of the wave through the interface. This reflected pulse has a limited high-frequency spectrum. The convolution in the time domain of this pulse with the reflection from any real dielectric (with relaxation) having a perfect interface gives the actual reflection obtained from a real dielectric with an extended interface. Errors introduced in the measurement of high-frequency permittivity and relaxation time can be eliminated by terminating the sample cell with plastic or ceramic beads similar to the ones shown in Figure 3.1. These beads have inner and outer conductor dimensions that produce a characteristic impedance of 50 ohms. They are, therefore, electrically in no way different from the remainder of the empty coaxial line but form a perfect physical interface with any liquid in contact with them.

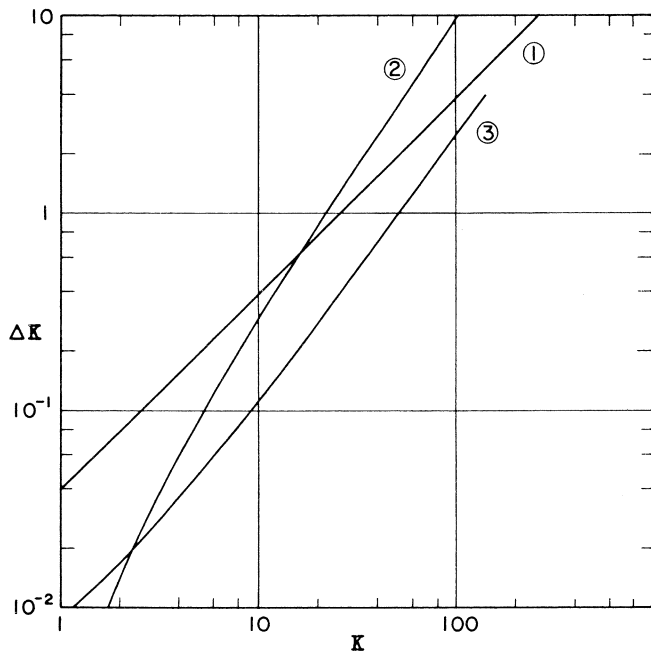


Figure 2.13 Different contributions to the absolute measurement of permittivity,  $\Delta\kappa$ .

- 1) Error due to dimensional tolerance of a 7mm precision air line.
- 2) Error due to the relative measurement error of reflection coefficient,  $\Delta\rho/\rho = 0.01$ .
- 3) Error due to noise and unwanted reflections,  $\Delta\rho = 2 \cdot 10^{-3}$ .

Finally, we shall consider the influence of the finite risetime of a step pulse on the measurement of  $\kappa_\infty$ , the high frequency permittivity. The pulse produced by the tunnel diode generator approximates a linear voltage ramp that rises from zero to  $V_0$  within the time  $t_r$ . This ramp is the integral of a step pulse and the response of the dielectric becomes the integral of the step pulse response divided by  $t_r$

$$f(t)_{\text{ramp}} = \frac{1}{t_r} \int f(t)_{\text{step}} dt$$

Thus, the derivative of the measured time response of the reflection coefficient during the risetime of pulse times  $t_r$  gives the response to a step pulse. In most cases investigated to date, the slope is practically constant, as shown in Fig. 2.14. The linear extrapolation of  $\rho$  to time  $t_r$  gives  $\rho_\infty$  and, from equation (2.6),  $\kappa_\infty$ .

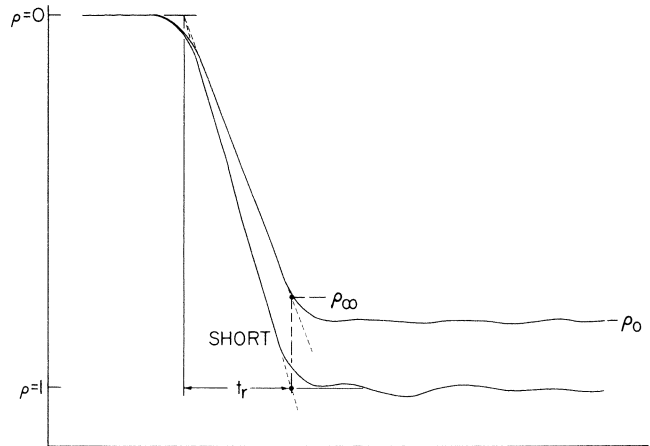


Figure 2.14 Determination of  $\rho_\infty$  for a pulse with finite risetime. It is obtained by extrapolation of the linear part of the curve to time  $t_r$ .

### 3. PRACTICAL ASPECTS OF THE TDR MEASUREMENTS.

#### SAMPLE CELLS

A simple and versatile cell for measurements of liquids and granular solids is the standard 7 mm diameter precision coaxial line of 10 and 20 cm length with Amphenol APC-7 connectors (see Figure 3.1).

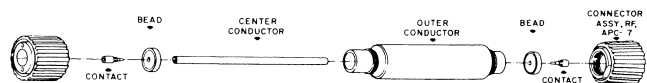


Figure 3.1 7mm precision air line. It is simple, accurate, and useful for many applications.

As previously mentioned, the maximum deviation from the 50 ohm impedance is  $\pm 0.2\%$ . The plastic bead on each end is machined accurately enough to provide a liquid-tight seal for a few hours. The plastic may be replaced with any ceramic material, such as alumina, for operation at temperatures above  $80^\circ\text{C}$  or to provide resistance against attack by organic solvents. The assembly, including the center conductor, is held in place on one side by the APC-7 connector, to allow filling the line from the other end. The hybrid connector is of high quality and does not introduce any significant reflections up to 18 GHz.

A number of solid brass beads, of the same dimension as the plastic beads were machined and silver plated to act as a short on one end of the sample line. For the measurement of the dielectric material the line is connected with the short on the far end from the pulse generator. The line is then turned around to measure the reference pulse from a short in about the same location as the interface air-dielectric was before.

For measurements at controlled temperatures, the sample cell may be connected on each side with another empty coaxial line, wrapped tightly in plastic or aluminum foil and surrounded by a water jacket that is connected to a temperature bath. The water jacket should extend at least 10 cm over each end of the empty line to insure uniform temperature in the sample. For measurements with liquids at low temperatures, the coaxial line should be mounted vertically and the signal supplied from the bottom to preserve a well defined interface between dielectric and air when the sample contracts during cooling.

Solids can be measured in a coaxial cell by filling the line with molten material, if possible, or by machining the substance to the dimension of the line, or by wrapping it tightly around the center conductor when available as foil, or by shredding or granulating it. TDR measures an average value of the permittivity if a line is not completely filled with a dielectric. Therefore, for absolute measurements the fill factor has to be known. Relative measurements of dielectric constant and exact determinations of relaxation time can be made, however, if the fill factor is unknown but constant. A change in packing density of the material over the length of the line will cause unwanted reflections from any point where a change in impedance occurs.

The dielectric properties of large batches of liquids may be measured with a vertical coaxial line immersed in the substance. Since the characteristic impedance,  $Z_0$ , depends only on the ratio of the diameters of inner and outer conductor, the line can be made any size, for mechanical stability, as long as no higher modes than the TEM mode are excited. A tapered 50 ohm section should be used to connect it to the standard coaxial line to avoid reflections. Small holes may be drilled at the upper end to allow the liquid in the measuring line to communicate with the outside. Still better exchange between inside and outside can be achieved by using a wire mesh as an outer conductor. The mesh acts as a homogeneous conductor if the holes in the mesh are small compared to the spatial resolution of the TDR. A continuous monitoring of chemical reactions by measuring the permittivity in a time interval where it is most sensitive to changes in the chemical composition is entirely feasible. In addition, the surface position of the liquid can be measured to provide a simple liquid level control. This application was suggested long ago<sup>(1)</sup> and has already found some practical use.

(1) J. Brockmeier, Hewlett-Packard Journal Vol. 17, No. 5 (1966).

The only limitation of the straight coaxial line is its length. A standard 7 mm line becomes quite unstable if more than 30 cm long due to vibrations and sagging of the center conductor. The line can be supported with one or two thin (0.5 mm) washers of mica without introducing serious reflections but such lines become unwieldy if they are longer than 50 cm. On the other hand, one great advantage of dielectric measurements with TDR is the freedom from multiple reflections if we measure only within the time for the return trip of the wave in the sample cell (see Part 2). A 40 cm long line, filled with a dielectric of  $\kappa = 20$  limits the range to  $< 12$  ns.

One way to make long compact coaxial lines is shown in Figure 3.2. Spiral grooves have been cut into a copper tube of 8 cm diameter. An extruded polypropylene spacer fits tightly into the grooves and supports a copper wire used as a center conductor. An outer tube fits closely over the inner one. Both tubes are sealed to a bottom plate, forming a rectangular coaxial line of 7 m length which can be filled from the top and immersed in a temperature bath. The empty line has 50 ohms impedance and a return trip time of about 50 ns. Because of the polypropylene spacer, the line has to be calibrated with known dielectrics. Relaxation times up to 200 ns have been measured which corresponds to 1 MHz in the frequency domain.

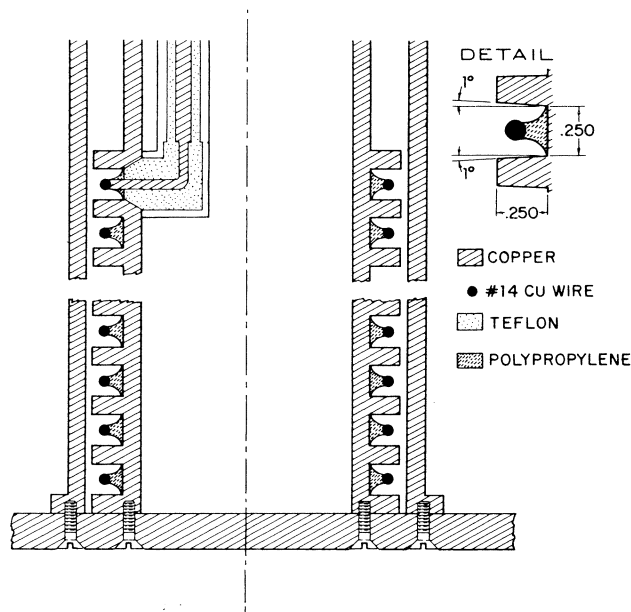


Figure 3.2 Helical coaxial line of 7m length. It is used mainly for the measurement of long relaxation times.

Another kind of transmission line well suited for many applications is the strip line. One of many possible configurations of such a line is shown in Figure 3.3. Two parallel, conductive strips were prepared by etching a printed circuit board. This line can be connected to a coaxial line with a balun transformer. Placing a piece of dielectric material over the two strips reduces the characteristic impedance of the

line and results in a dip of the oscilloscope trace. Since the test material fills only part of the field region, a calibration curve with known dielectrics has to be made. Once this is done, the relaxation properties of solids can be measured without much sample preparation. This method may be used as a simple and expedient check of dielectrics for quality control and similar applications. Also, multilayers of plastic foil, pressed against the two conductors, give rather reproducible readings.

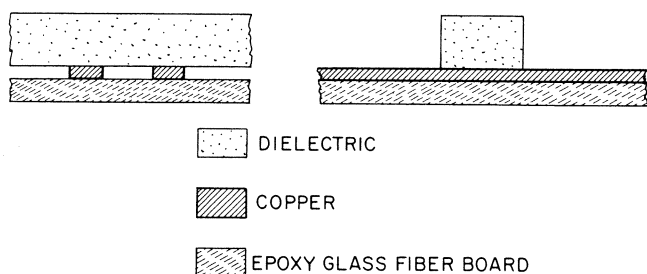


Figure 3.3 Sample testing with the strip line. The sample is placed across the two conducting strips. This method can be used for checking solid dielectric samples with a minimum of sample preparation.

#### MEASUREMENT TECHNIQUES

Some precautions are necessary to use the high sensitivity of TDR to its fullest advantage. One is the suppression of unwanted reflections, the other is the correction of slight pulse shape deviations from an ideal step pulse with a linear risetime. Interfering reflections may appear superimposed on the oscilloscope trace during the time interval in which the reflection coefficient  $\rho$  drops to its final value  $\rho_0$ . They may be small bumps when originating from local discontinuities or small steps when caused by extended impedance mismatches between pulse generator and sample. They are produced by the reflected pulse from the interface air-dielectric traveling towards the generator. Any poor connector in this path or even the small but finite impedance mismatch in the sample  $\gamma$  can produce such reflections. They can be spaced farther apart or suppressed by inserting about 40 cm of a precision air line between sampler and measuring cell. Also, a 10 dB attenuator in place of the air line effectively dampens reflections, however, the sensitivity is reduced. Placing a short in the place of the air-dielectric interface allows one to clearly examine these interferences. Figure 3.4 shows the trace of a short, 50 ohm-line, and a dielectric with a deliberately produced poor connection at the sampler.

The same figure also shows the slight pulse overshoot at the bottom of the step due to the sampler frequency response, and a certain slow droop to a final value. Both may cause measurement errors of high frequency permittivity  $\kappa_\infty$  and of relaxation time  $\tau$ . This interference can be eliminated by the following procedure: First, connect the measuring cell, with a short at the far end (as seen from the instrument), and record the

trace. Then, turn it around to have the short in front of the cell and record its trace on the same graph. Finally, substitute the cell by a precision air line and superimpose the traces (Figure 3.4). The true value of reflection coefficient  $\rho$  at any point in time is  $\rho_m/a$ .

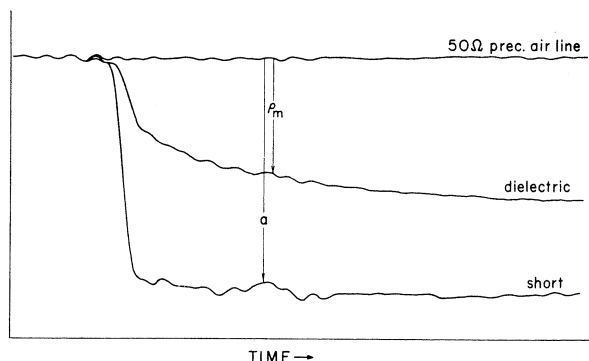


Figure 3.4 Trace of the reflection coefficient from a 50 ohm line, a dielectric and a short. Pulse shape imperfections and unwanted reflections can be corrected by measuring  $\rho_m$  and  $a$  at any point in time. The true value of the reflection coefficient  $\rho = \rho_m/a$ .

The measurement accuracy may be improved further for repeated measurements with materials of fairly constant permittivity by making the ratio of inner to outer diameter in a coaxial line smaller to give an impedance of about 50 ohms when filled with the dielectric. In Figure 2.13 we have shown for a standard 50 ohm coaxial line that the absolute measurement accuracy improves considerably for  $\kappa \rightarrow 1$ .

Relative measurements between a sample and a reference material can be made with the HP 1430A sampler with two sampling inputs which can be used simultaneously as shown in Figure 3.5 and 3.6. The two inputs from the sampler to the HP 1411A sampling amplifier can be displayed separately or one may be subtracted from the other. This feature is of particular interest since it allows extraction of small differences in the dielectric behavior between the sample and the reference due to impurities, reaction products, temperature, or other influences. Most errors or interferences cancel, and the ultimate measurement accuracy is determined by the noise level of the instrument.

#### APPLICATIONS

The greatest assets of this method are speed, simplicity, and ease of data evaluation. In the past, the ability to characterize dielectrics over a wide frequency range was limited to a few laboratories and the number of substances investigated was restricted by the time and effort required. Multiple reflections, which are ever present in measurements in the frequency domain, require careful attention and make data evaluation tedious. In contrast, the display on the oscilloscope screen of the time domain reflectometer is easy to interpret, displays immediate information about the behavior of the material investigated, and shows if the instrument is operating properly and if any unwanted reflections are present. The measurement

range for relaxation times of about 50 ps to 200 ns (corresponding to a frequency range of about 1 MHz to 3 GHz) covers a region of great interest. The accuracy, while not as good as obtainable in the frequency domain, may be sufficient for many applications and can be improved with special techniques mentioned earlier in this section.

A number of applications have been tried or were suggested by different people. The characterization of dielectric materials for quality control and incoming inspection can be done in very short time and with a minimum of sample preparation. The time scale and vertical sensitivity of the instrument can be adjusted to get an optimum display for each substance tested, and an overlay for the oscilloscope screen can be used to define the range of acceptance. The information content is high since three parameters are obtainable from one measurement:  $\epsilon_0$ ,  $\epsilon_\infty$ ,  $\tau$  or  $\sigma$ .

In many materials, the high frequency permittivity is quite sensitive to impurities of small free molecules, such as water, monomers; etc. These impurities have very short relaxation times...sometimes below the time resolution of the time domain reflectometer...and relatively high specific permittivities. On the other hand, host materials such as polymers have high frequency dielectric constants in the range of  $\epsilon_\infty = 2$  to 8. The high accuracy of TDR in this range (see Figure 2.13) allows the determination of less than 1000 ppm of water, which is of interest for the plastics industry. The difference measurement between a sample and a dry reference material makes this measurement still more sensitive. To our knowledge, there is no other simple and nondestructive method available for this test and continuous monitoring system for impurities is possible.

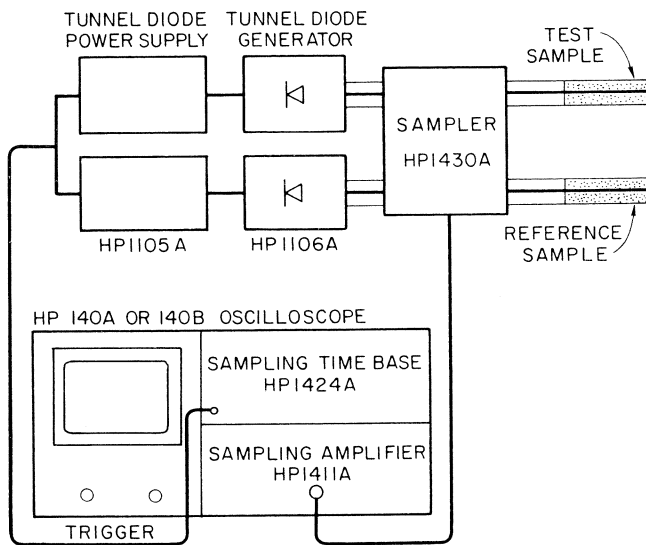


Figure 3.5 Differential TDR measurement with the HP 1430A sampler.

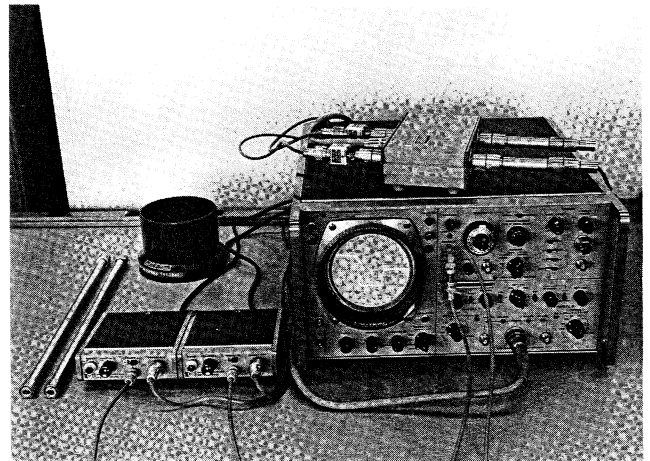


Figure 3.6 Differential TDR measurement with the HP 1430A sampler.

Since the measurement speed is essentially limited by the scan density and the pulse generator repetition rate, which is roughly 100 kHz when triggered from the sampling time base, very fast reactions can be monitored. Using the HP 141 or 181 variable persistence and storage oscilloscope instead of the 140 and adjusting the repetition rate of the pulse generator according to the reaction rate, allows storing a number of traces of the reflection coefficient vs. time on the oscilloscope screen and gives immediate information about changes taking place during the reaction. The stored traces can then be photographed and evaluated in detail.

A relatively slow reaction which has been observed with TDR is the polymerization of epoxy resins inside a coaxial line. Figures 3.7 and 3.8 show the time dependence of the dielectric constant and relaxation time for different polymerization times. The strong change of the static permittivity  $\kappa_0$  with time at short polymerization times is due to the free rotation of the monomer of the epoxide (glycerin diepoxide) and the catalyst (aliphatic diamine). This change becomes less

as the polymerization progresses. Also, the high frequency dielectric constant changes with time indicating that the amino- and oxy-groups of the monomers, which have very short relaxation times, are reacting during the polymerization. The difference between the dielectric constant in the infrared region and the measured  $\kappa_\infty$  of the fully polymerized material gives further information about the structure of this resin. Obviously, TDR can be applied in a similar way for monitoring chemical reactions on a production scale.

Dielectrics with high loss are difficult to measure at microwave frequencies. TDR measures the permittivity and conductivity from the internal relaxation time

$$\tau = \frac{\epsilon [\text{Fcm}^{-1}]}{\sigma [\Omega^{-1}\text{cm}^{-1}]} = \frac{1.1 \cdot 10^{-12} \kappa}{4\pi \sigma}$$

in the same manner as dielectric relaxation. Highly conductive solutions of ions in polar organic solvents can be determined without difficulty. An example is Figure 2.12.

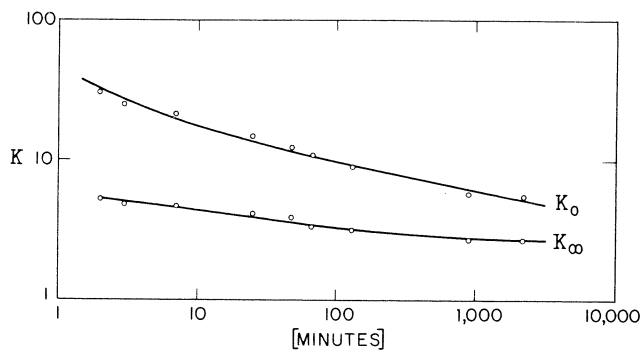


Figure 3.7 Polymerization of glycerin diepoxide with an aliphatic diamine: High Frequency and static permittivity vs. polymerization time. This resin appeared hard after 1 hour, yet some reaction is still going on after 15 hours.

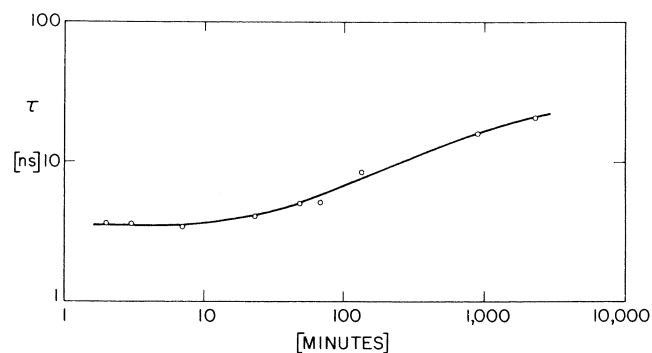


Figure 3.8 Polymerization of glycerin diepoxide with an aliphatic diamine: The relaxation time goes up as the monomers polymerize and form, on the average, dimers, trimers, and so on.

## APPENDIX I

## THE CORRELATION BETWEEN TIME AND FREQUENCY DOMAIN

It is well known that distortion of a sinusoidal signal, with its signal power concentrated at one frequency  $\omega_0$ , produces harmonic frequencies  $m\omega_0$ , thus distributing the power over a certain frequency range. In a more general way, we can state that any time dependent signal can be expressed in terms of its frequency spectrum. The quantitative correlation between the time domain and the frequency domain is given by Fourier or Laplace transform. We will use the Laplace transform, which is more appropriate for time domain reflectometry, and will give a few basic facts which may help to understand the dielectric measurements in the time domain. The reader may consult any one of a number of books on transform calculus for a deeper understanding.

The transform from the time domain into the frequency spectrum is given by

$$F(\omega) = \int_0^{+\infty} f(t) \cdot e^{-i\omega t} dt \quad (1)$$

As an example, we will make the Laplace transform of a square pulse train with pulse length  $t_1$ , repetition time  $t_0$ , and unity amplitude. The integral then becomes

$$F(\omega) = \sum_{n=0}^{+\infty} \int_{nt_0}^{nt_0+t_1} e^{-i\omega t} dt \quad (2)$$

since  $f(t) = 1$  for every time interval  $t_1$ , starting at  $n \cdot t_0$ , and  $f(t) = 0$  for the remainder of the time. Thus

$$\begin{aligned} F(\omega) &= \frac{i}{\omega} \sum_{n=0}^{+\infty} e^{-i\omega t} \left[ \begin{array}{l} nt_0 + t_1 \\ nt_0 \end{array} \right] \\ &= \frac{i}{\omega} (e^{-i\omega t_1} - 1) \sum_{n=0}^{+\infty} e^{-in\omega t_0} \end{aligned}$$

Since

$$\begin{aligned} & i (\exp(-i\omega t_1) - 1) \\ &= 2 \frac{\left( \exp\left(\frac{i\omega t_1}{2}\right) - \exp\left(\frac{-i\omega t_1}{2}\right) \right) \exp\left(\frac{-i\omega t_1}{2}\right)}{2i} \\ &= 2 \sin \frac{\omega t_1}{2} \cdot \exp\left(\frac{-i\omega t_1}{2}\right) \end{aligned}$$

we get

$$|F(\omega)| = \frac{2}{\omega} \sin \frac{\omega t_1}{2} \sum_{n=0}^{n=+\infty} e^{-in\omega t_0} \quad (3)$$

The summation term in equation (3) is different from zero only for  $\omega t_0 = 2\pi m$  ( $m = 1, 2, 3, \dots$ ) or

$$f_{m-1} = \frac{\omega}{2\pi} = \frac{m}{t_0} \quad (4)$$

Equation (4) represents the fundamental frequency  $f_0 = \frac{1}{t_0}$  and its harmonics. Their amplitude distribution is given by the absolute value of the complex term in equation (3). Thus

$$|F(\omega)| = t_1 \cdot \frac{\sin \frac{\omega t_1}{2}}{\frac{\omega t_1}{2}} \quad (5)$$

The frequency spectrum envelope corresponding to a single step of unit height at  $t = 0$  is

$$F(\omega) = \int_0^{\infty} e^{-i\omega t} dt = \frac{1}{i\omega} \quad (6)$$

$$|F(\omega)| = \frac{1}{\omega}$$

The frequency spectrum of the square pulse train, according to equation (3), is given in Figure AI-1d. We can draw a number of important conclusions:

1. The spectrum contains only the fundamental frequency and its harmonics. Pulse spacing depends only on the repetition time  $t_0$  of the pulse train. The lower the repetition rate the closer the spacing (see Figure AI-1e). Therefore, the spectrum of a single pulse becomes a continuum.
2. The nodes in the amplitude distribution depend only on the pulse length  $t_1$  and move closer together for longer pulses.

3. A fast risetime pulse contains higher harmonics than a slow risetime pulse and can be seen by comparing the spectrum of a rectangular and of a triangular pulse in Figure AI-1c. It becomes even clearer in Figure AI-2 where we have plotted the frequency spectrum of single pulses of finite and infinite length with different risetimes.

4. The high frequency part of the spectrum depends on the shape of the pulse in the vicinity of  $t = 0$  and vice versa. In Figure AI-2, the high frequency spectrum of pulses is identical if the risetime at the start of the pulse is the same. Therefore, approximations for certain spectral ranges can be made if it is difficult to obtain the Laplace transform for the entire pulse.

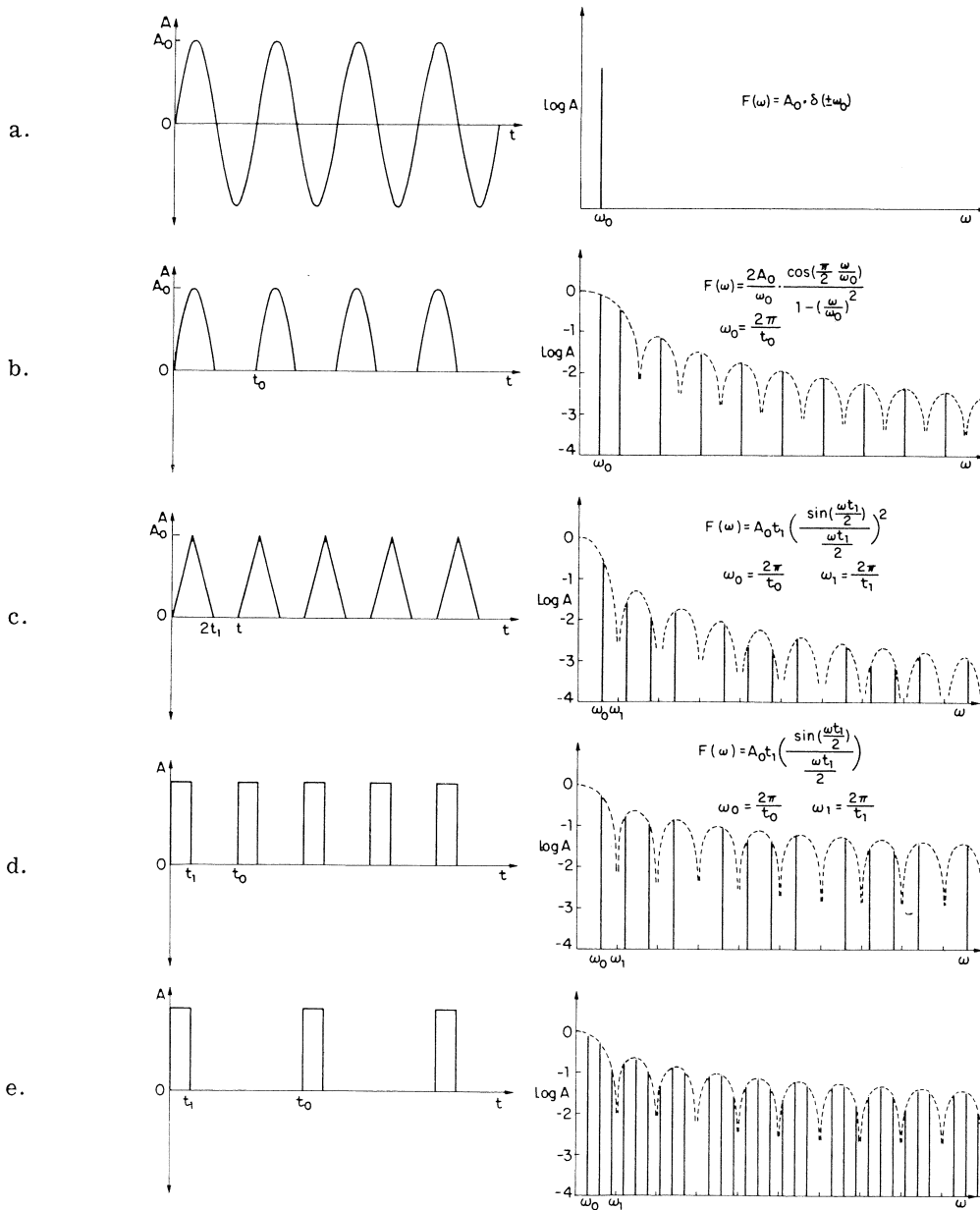


Figure AI-1 Frequency spectrum of various pulse trains

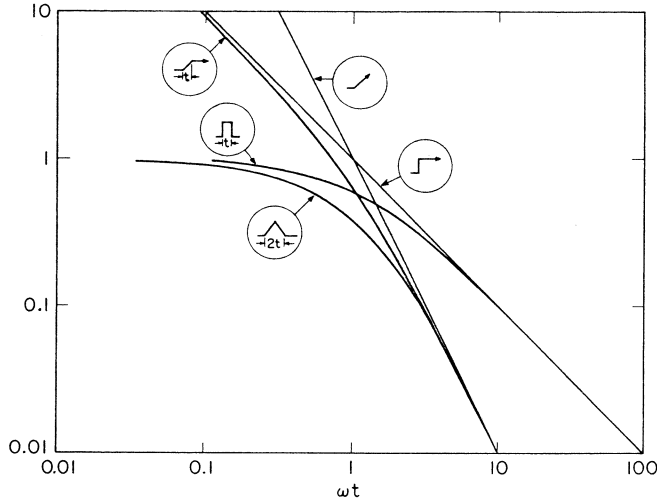


Figure AI-2 Frequency spectrum of single pulses of unit height and/or unit slope with  $t = 1$ .

We have used one other theorem in the text which is explained briefly: The frequency response  $H(\omega)$  of any system to an input signal  $G(\omega)$  can be represented by its transfer function  $F(\omega)$  which is

$$H(\omega) = G(\omega) \cdot F(\omega)$$

Laplace transform into the time domain gives

$$h(t) = g(t) * f(t) = \int_{\tau=0}^t f(\tau) \cdot g(\tau - t) d\tau. \quad (7)$$

The simple product of input signal with the transfer function in the frequency domain becomes a convolution in the time domain. However, for an infinitely short pulse of unit area ( $\delta$ -function) the convolution integral in equation (7) becomes

$$h(t) = \int_{\tau=0}^t f(\tau) \cdot \delta(\tau - t) d\tau = f(t)$$

since

$$\int \delta(\tau - t) = 0 \text{ for } \tau = t \text{ and} \\ 1 \text{ for } \tau = t.$$

The frequency spectrum of the  $\delta$ -function is constant and unity, giving

$$H(\omega) = F(\omega) \cdot \delta(\omega) = F(\omega).$$

The integral of  $\delta(t)$  is a step pulse,  $u(t)$ , with infinitely short risetime and unit height.  $\int u(t)dt$  in turn is a ramp,  $s(t)$ , with unit slope. Also the transform of an integral

$$f(t) = \int f'(t) dt \quad \text{is}$$

$$F(\omega) = \frac{1}{\omega} F'(\omega),$$

the transform of the integrand divided by  $\omega$ . Since  $\delta(\omega) = 1$ , we get  $u(\omega) = \frac{1}{\omega}$  and  $s(\omega) = \frac{1}{\omega^2}$ . This means,

however, that the response of a system to a step pulse

$$H(\omega)_{\text{step}} = \frac{1}{\omega} \cdot F(\omega) \quad \text{is} \quad (8)$$

$$h(t)_{\text{step}} = \int f(t)_{\delta} dt,$$

the integral of the system response. And, consequently,

$$h(t)_{\text{ramp}} = \iint f(t)_{\delta} dt^2. \quad (9)$$

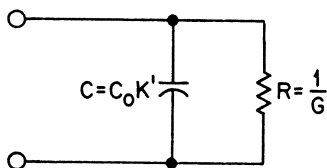
We used equations (8) and (9) in computing the response of a dielectric to a step pulse and to a pulse with linear risetime.

## APPENDIX II

### THE PRINCIPLE OF DIELECTRIC MEASUREMENTS

Many measurements of dielectric properties, particularly at low frequencies, are made by measuring the impedance of a capacitor with and without the test material between the two plates. A number of measurements at different frequencies over a wide range are required for the characterization of dielectrics.

The equivalent circuit for a capacitor filled with a dielectric is



The admittance  $Y$  ( $= 1/Z$ ,  $Z$ : impedance) of this circuit is

$$Y = j2\pi fC + G = j\omega C + G = jB + G \quad \begin{array}{l} B : \text{Susceptance} \\ G : \text{Conductance} \end{array}$$

The admittance of the same capacitor without dielectric would be

$$Y_0 = j\omega C_0$$

The dielectric changes  $Y_0$  to  $Y$ . Therefore, we multiply  $Y_0$  with a complex factor, the permittivity  $\kappa^* = \kappa' + j\kappa''$ , to get  $Y$ :

$$\begin{aligned} Y &= \kappa^* \cdot Y_0 = (\kappa' - j\kappa'') Y_0 \\ &= j\omega C_0 (\kappa' - j\kappa'') \quad (5) \\ &= j\omega \kappa' C_0 + \omega \kappa'' C_0 \\ &= j\omega C + G \end{aligned}$$

and

$$\begin{aligned} C = \kappa' C_0 \quad \text{or} \quad \kappa' &= \frac{C}{C_0} \\ G = \omega \kappa'' C_0 \quad \kappa'' &= \frac{G}{\omega C_0} \end{aligned} \quad (6)$$

$$G [\Omega^{-1}]$$

$$C, C_0 [\text{Farad}]$$

The dielectric constant  $\kappa'$  is a measure of the degree of electrical polarization in the material, due either to formation of dipoles by induced polarization or the orientation of permanent dipoles. This polarization in an electric field produces free charges at the surface of the material which, in turn, tends to reduce the electric field inside the material. The surface charge density  $P$  is given by

$$P = E(\kappa' - 1) \quad (7)$$

The dielectric loss may be due either to conductivity (electronic or ionic) in material or to energy dissipation of rotating permanent dipoles in an alternating field. For the former, the conductance can be simply related to the conductivity ( $\sigma$ ) of the material by

$$\frac{G}{C_0} = 4\pi\sigma = 4\pi/\rho = \omega\kappa''$$

since (for a plate capacitor)

$$G = \sigma \cdot \frac{A}{d} [\Omega^{-1}] \quad C_0 = \frac{A}{4\pi d} [\text{cm}].$$

$\rho$  : resistivity

$A$  : area of plates

$d$  : spacing between plates

The theory for the behavior of permanent dipoles has been developed by Debye<sup>(1,2)</sup> and Onsager<sup>(3)</sup>, using in part Langevin's<sup>(4)</sup> theory of permanent magnetic dipoles. We can give the results only and have to refer the reader to the literature for further details:

At low frequencies the dipoles will have time enough to orient themselves in the electric field, giving a high dielectric constant. At high frequencies, the dipoles cannot follow the fast changing field; they remain randomly oriented and do not contribute to the dielectric constant. The transition occurs in the vicinity of a certain frequency  $2\pi f_0 = \omega_0$  and at this

(1) P. Debye, Phys. Z. B, 97 (1912).

(2) P. Debye, Polar Molecules, Dover Publ., N.Y.

(3) L. Onsager, J. Am. Chem. Soc. 58, 1486 (1936).

(4) M.P. Langevin, J. Physique 4, 678 (1905).

frequency, the dielectric loss has a maximum value. The solution of the differential equation

$$\mu E e^{j\omega t} \cos \theta - \eta \frac{d\theta}{dt} = 0 \quad (8)$$

$\theta$  : angle between dipole and field E  
 $\mu$  : dipole moment  
 $\eta$  : friction constant

with appropriate boundary conditions and for an electric field  $E < \frac{\mu}{KT}$  [corresponding to  $< 10^7$  V/cm at room temperature and  $\mu = 1$  (Debye) ] gives

$$\kappa^*(\omega) = \kappa'(\omega) + j\kappa''(\omega) = \kappa_\infty + \frac{(\kappa_0 - \kappa_\infty)}{(1 + j\omega\tau)} \quad (9)$$

$\kappa'_0$  : low frequency dielectric constant  
 $\kappa'_\infty$  : high frequency dielectric constant

After separation into real and imaginary parts one gets

$$\kappa'(\omega) = \kappa_\infty + \frac{\kappa_0 - \kappa_\infty}{1 + \omega^2 \tau^2} \quad (10)$$

$$\kappa''(\omega) = \frac{(\kappa_0 - \kappa_\infty) \cdot \omega\tau}{1 + \omega^2 \tau^2} \quad \tau : \text{relaxation time} \quad (11)$$

This function is shown in Figure AII-1.

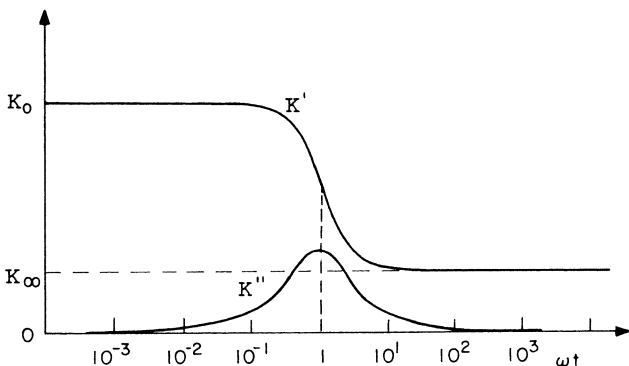
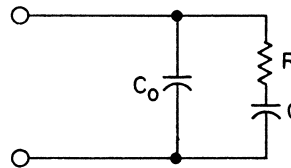


Figure AII-1 Real and imaginary part of the permittivity,  $\kappa'$  and  $\kappa''$  respectively, vs. frequency.

The equivalent circuit for a capacitor filled with such a dielectric is



The Laplace transform of equation (9) gives

$$\kappa(t) = \frac{(\kappa_0 - \kappa_\infty)}{\tau} e^{-\frac{t}{\tau}} \quad (12)$$

which is the response of the permittivity to an infinitely short voltage impulse whose time integral is unity ( $\delta$ -function) and which produces the permittivity  $\kappa_0$ . The contribution to capacitance due to the permittivity  $\kappa_\infty$  decays immediately, while  $(\kappa_0 - \kappa_\infty)$  decays according to (12).

It comes closer to a practical approach to consider the response of the system to a voltage step pulse  $u(t)$  which is the integral of a  $\delta$ -function ( $u(t) = 0$  for  $t < 0$ ,  $u(t) = 1$  for  $t > 0$ ). Therefore, the time response of permittivity is the integral of equation (12). We get

$$\kappa(t) = \kappa_\infty + (\kappa_0 - \kappa_\infty) (1 - e^{-\frac{t}{\tau}}) \quad \text{with } \kappa(0) = \kappa_0 \quad (13)$$

see Figure AII-2.

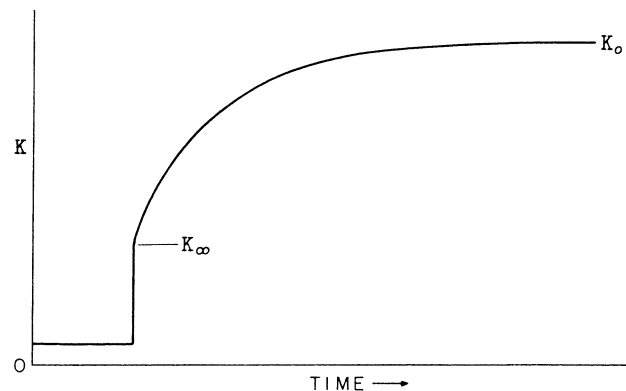


Figure AII-2 Step response of the permittivity of an ideal dielectric.

The curve starts at  $\kappa_{\infty}$ , since we assume that the time constant of this contribution to permittivity is very small compared with the time scale used. The permittivity then rises to  $\kappa_0$  with the time constant  $\tau$ .

There may be other dispersion regions of the permittivity. Particularly at short relaxation times there may be fast orientation polarization of small dipoles, induced or dipole orientation of atoms, and induced electron polarization. All these contribute to  $\kappa_{\infty}$ , the high frequency permittivity. The following table gives some information about relaxation time, frequency, and wavelength range where these processes occur (for Debye behavior).

Whenever there is an interaction between the oriented group or molecule and the surrounding medium, the viscosity will have an influence on the relaxation time. Since the viscosity of solids and liquids is

strongly temperature dependent, the relaxation time of the first three groups also shows strong temperature dependence. Functional groups are generally small enough to move within the sphere in influence of their own molecule and the viscosity loses its meaning.

It may be pointed out now that the Hewlett-Packard Time Domain Reflectometer covers a range of  $3 \cdot 10^{11}$  to  $10^{-6}$  seconds which allows measuring the orientation of molecules and some functional groups in solids and liquids. This is a region of great theoretical and practical interest. Longer relaxation times can be measured with rather simple bridge and pulse circuits. It would be desirable to be able to measure relaxation times of a few picoseconds with TDR for identification of specific functional groups. At the moment, there is no indication that this will be possible soon and such measurements have to be made in the frequency domain.

TABLE AII-1

| Relaxation Mechanism                                     | Relaxation Time [sec]                          | Frequency [ $\text{sec}^{-1}$ ]       | Wavelength [cm]                     | Temp. Depend. of Relax. Time |
|--|--|---------------------------------------|-------------------------------------|------------------------------|
| 1) Orientation of molecular (?) groups in solid polymers | $10^4 - 10^{-4}$                               | $1.6 \cdot 10^{-5} - 1.6 \cdot 10^3$  | $2 \cdot 10^{15} - 2 \cdot 10^7$    | Strong                       |
| 2) Orientation of functional groups in solids            | $10^{-5} - 10^{-11}$                           | $1.6 \cdot 10^4 - 1.6 \cdot 10^{10}$  | $2 \cdot 10^6 - 2$                  | Medium                       |
| 3) Orientation of molecules in liquids                   | $10^{-6} - 10^{-11}$                           | $1.6 \cdot 10^5 - 1.6 \cdot 10^{10}$  | $2 \cdot 10^5 - 2$                  | Strong                       |
| 4) Orientation of functional groups in liquids           | $10^{-9} - 10^{-12}$                           | $1.6 \cdot 10^8 - 1.6 \cdot 10^{11}$  | $2 \cdot 10^2 - 0.2$                | Small                        |
| 5) Orientation of molecules in gases                     | $10^{-8} - 10^{-12}$                           | $1.6 \cdot 10^7 - 1.6 \cdot 10^{11}$  | $2 \cdot 10^3 - 0.2$                | Small                        |
| 6) Atom polarization (rotational and vibrational)        | $5 \cdot 10^{-16} - 10^{-14}$                  | $3 \cdot 10^{14} - 1.5 \cdot 10^{13}$ | $10^{-4} - 2 \cdot 10^{-3}$         | None                         |
| 7) Electron polarization                                 | $1.6 \cdot 10^{-16}$<br>$- 1.6 \cdot 10^{-15}$ | $10^{15} - 10^{14}$                   | $3 \cdot 10^{-5} - 3 \cdot 10^{-4}$ | None                         |

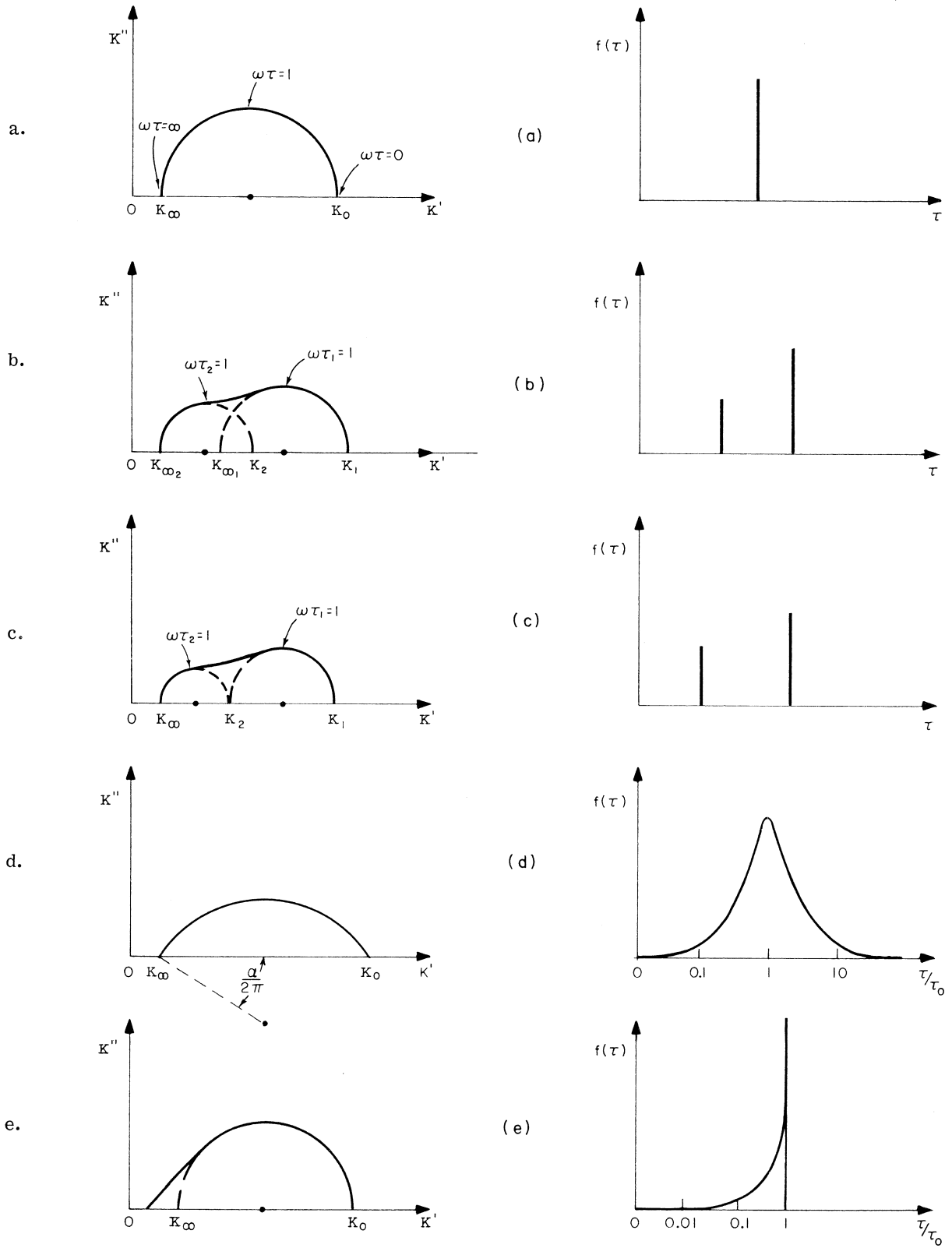


Figure AII-3 Cole & Cole diagram of relaxation spectrum for different types of dielectrics.

In the case of time domain reflectometry the Laplace transform of the reflection coefficient has to be made, as mentioned on Page 5. The mathematical treatment for Debye dielectrics<sup>(5)</sup> are given by H. Fellner-Feldegg and F. Barnett.

The differential equation (8) assumes a single and constant dipole moment and friction constant, resulting in one single relaxation time. If there are two independent relaxation times of about the same magnitude in one substance or in a mixture of two species, then the permittivity is given as a linear addition of two terms with relaxation times  $\tau_1$  and  $\tau_2$  in equation (9). This addition is preserved when making the transform into the frequency domain. Thus

$$\chi^*(\omega) = \chi_\infty + \frac{\chi_1 - \chi_\infty}{1 + j\omega\tau_1} + \frac{\chi_2 - \chi_\infty}{1 + j\omega\tau_2} \quad (14)$$

$$\chi(t) = \chi_\infty + (\chi_1 - \chi_\infty) \left(1 - e^{-\frac{t}{\tau_1}}\right) \quad (15)$$

$$+ (\chi_2 - \chi_\infty) \left(1 - e^{-\frac{t}{\tau_2}}\right)$$

In the frequency domain, Cole & Cole<sup>(6)</sup> have shown that the real and imaginary part of the permittivity, plotted in the complex plane for different frequencies, gives a semicircle for ideal Debye relaxation (see Figure AII-3a). Consequently, for the case of two independent relaxation times, one gets a plot shown in Figure 3b. Figure 3c shows the Cole & Cole plot for a substance with two well separated relaxation times, for example, an aliphatic alcohol. In the time domain, the logarithmic plot results in two straight lines with entirely different slopes.

If inter- and intramolecular interactions become important, then single relaxation times broaden into relaxation spectra. Fuoss and Kirkwood<sup>(7)</sup> and Cole<sup>(8)</sup> assume a relaxation spectrum which is symmetrical on a logarithmic scale about a central relaxation time  $\tau_0$ . The empirical equation of Cole fits the data to an arc of a circle in the Cole & Cole diagram and is of the form

$$\chi^*(\omega) = \chi_\infty + \frac{\chi_0 - \chi_\infty}{1 + (j\omega\tau_0)^{1-\alpha}} \quad (16)$$

Finally, glycerol and other substances show a highly asymmetric Cole & Cole diagram, described by Davidson & Cole<sup>(9)</sup> (Figure 3e) with

$$\chi^*(\omega) = \chi_\infty + \frac{\chi_0 - \chi_\infty}{(1 + j\omega\tau_0)^\beta} \quad (17)$$

(5) H. Fellner-Feldegg, F. Barnett  
J. Phys. Chem. 74, (July 1970).

(6) K. S. Cole, R. H. Cole, J. Chem.  
Phys. 9, 341 (1941).

(7) R. M. Fuoss, J. G. Kirkwood, J. Am. Chem.  
Soc. 63, 385 (1941).

(8) R. H. Cole, J. Chem. Phys. 23, 493 (1955).

(9) D. W. Davidson, R. H. Cole, J. Chem. Phys.  
19, 1484 (1951).



For more information, call your local HP Sales Office or East(201) 265-5000 . Midwest (312) 677-0400 . South (404) 436-6181  
West (213) 877-1282. Or, write: Hewlett-Packard, 1501 Page Mill Road, Palo Alto, California 94304. In Europe, 1217 Meyrin-Geneva